

# Long-Term Engraftment and Fetal Globin Induction upon *BCL11A* Gene Editing in Bone-Marrow-Derived CD34<sup>+</sup> Hematopoietic Stem and Progenitor Cells

Kai-Hsin Chang,<sup>1</sup> Sarah E. Smith,<sup>1,3</sup> Timothy Sullivan,<sup>1,3</sup> Kai Chen,<sup>1</sup> Qianhe Zhou,<sup>1</sup> Jason A. West,<sup>1</sup> Mei Liu,<sup>1</sup> Yingchun Liu,<sup>1</sup> Benjamin F. Vieira,<sup>1</sup> Chao Sun,<sup>1</sup> Vu P. Hong,<sup>1</sup> Mingxuan Zhang,<sup>1</sup> Xiao Yang,<sup>1</sup> Andreas Reik,<sup>2</sup> Fyodor D. Urnov,<sup>2</sup> Edward J. Rebar,<sup>2</sup> Michael C. Holmes,<sup>2</sup> Olivier Danos,<sup>1</sup> Haiyan Jiang,<sup>1</sup> and Siyuan Tan<sup>1</sup>

<sup>1</sup>Biogen, Cambridge, MA 02142, USA; <sup>2</sup>Sangamo BioSciences, Richmond, CA 94804, USA

**To develop an effective and sustainable cell therapy for sickle cell disease (SCD), we investigated the feasibility of targeted disruption of the *BCL11A* gene, either within exon 2 or at the GATAA motif in the intronic erythroid-specific enhancer, using zinc finger nucleases in human bone marrow (BM) CD34<sup>+</sup> hematopoietic stem and progenitor cells (HSPCs). Both targeting strategies upregulated fetal globin expression in erythroid cells to levels predicted to inhibit hemoglobin S polymerization. However, complete inactivation of *BCL11A* resulting from bi-allelic frameshift mutations in *BCL11A* exon 2 adversely affected erythroid enucleation. In contrast, bi-allelic disruption of the GATAA motif in the erythroid enhancer of *BCL11A* did not negatively impact enucleation. Furthermore, *BCL11A* exon 2-edited BM-CD34<sup>+</sup> cells demonstrated a significantly reduced engraftment potential in immunodeficient mice. Such an adverse effect on HSPC function was not observed upon *BCL11A* erythroid-enhancer GATAA motif editing, because enhancer-edited CD34<sup>+</sup> cells achieved robust long-term engraftment and gave rise to erythroid cells with elevated levels of fetal globin expression when chimeric BM was cultured *ex vivo*. Altogether, our results support further clinical development of the *BCL11A* erythroid-specific enhancer editing in BM-CD34<sup>+</sup> HSPCs as an autologous stem cell therapy in SCD patients.**

## INTRODUCTION

Sickle cell disease (SCD) is caused by an A → T mutation that changes the negatively charged glutamic acid to hydrophobic valine in position 6 (E6V) of the β-globin subunit of adult hemoglobin (HbA). When deoxygenated, hydrophobic patches of sickle hemoglobin (HbS) molecules interact with each other, forming tubular HbS fibers that increase the rigidity of the red blood cells (RBCs). Sick RBCs (ss-RBCs) have a shortened lifespan in the circulation; they adhere to and activate endothelium, promote inflammation, and interact with leukocytes, leading to episodes of painful sickle cell crisis and progressive organ damage.<sup>1,2</sup> SCD treatment is mainly supportive and focuses on alleviating disease complications. Hydroxyurea, which induces fetal γ-globin<sup>3</sup> and inhibits HbS polymerization,<sup>4–6</sup> is the only approved drug for managing SCD with demonstrated re-

ductions in morbidity and mortality.<sup>7,8</sup> However, concerns about its potential carcinogenic properties have contributed to its underuse.<sup>9</sup> Current life expectancy of patients with sickle cell anemia in the United States is roughly three decades shorter than that of the general population.<sup>10,11</sup>

Allogeneic hematopoietic stem cell (HSC) transplant (HSCT) can be curative for SCD, but only 18% of SCD patients have matched sibling donors.<sup>12</sup> Receiving a graft from an unmatched donor is associated with a higher risk for mortality and morbidity.<sup>13</sup> Clinical trials utilizing autologous bone marrow (BM) CD34<sup>+</sup> cells transduced with lentiviral vectors carrying anti-sickling globin genes are currently under way, but so far have been met with mixed outcomes.<sup>14–16</sup> Another lenti-based short hairpin RNA (shRNA) gene therapy approach that selectively knock downs B cell lymphoma/leukemia 11A (*BCL11A*), one of the key suppressors of anti-sickling fetal γ-globin,<sup>17–20</sup> in erythroid cells is actively under investigation.<sup>21,22</sup> Other novel gene therapy strategies such as correcting the sickle mutation in induced pluripotent stem cells (iPSCs)<sup>23,24</sup> or in primary human CD34<sup>+</sup> hematopoietic stem and progenitor cells (HSPCs)<sup>25,26</sup> have been explored pre-clinically. However, fully functional HSCs have yet to be derived from iPSCs,<sup>27</sup> and achieving efficient levels of gene correction in long-term repopulating HSCs via homology-directed repair (HDR) pathways without utilizing a selectable marker<sup>26</sup> has remained challenging,<sup>28</sup> limiting the clinical relevance of such approaches. In contrast to HDR, gene disruption via non-homologous end joining (NHEJ) repair pathways occurs at a high frequency in HSCs.<sup>28</sup> Therefore, reactivating fetal γ-globin while reducing sickle adult β-globin expression via the disruption of *BCL11A*, whose only known function in the erythroid lineage appears to be mediating fetal to adult globin switching,<sup>17,18,29,30</sup> offers a potential strategy for developing an effective treatment for SCD.

Received 1 October 2016; accepted 28 December 2016;  
<http://dx.doi.org/10.1016/j.omtm.2016.12.009>.

<sup>3</sup>These authors contributed equally to this work.

**Correspondence:** Kai-Hsin Chang, Biogen, Cambridge, MA 02142, USA.  
**E-mail:** [kaihsin.chang@biogen.com](mailto:kaihsin.chang@biogen.com)



Here, we employed zinc finger nucleases (ZFNs) to disrupt expression of the *BCL11A* gene in BM-derived CD34<sup>+</sup> cells from healthy volunteers. Through a combination of in vitro and in vivo studies, we show that targeted disruption of the GATAA motif in the erythroid-specific enhancer of *BCL11A* can both reactivate fetal  $\gamma$ -globin to levels expected to prevent HbS polymerization and produce edited HSPCs capable of long-term multilineage engraftment in immunodeficient mice. Together, these data provide a compelling rationale to pursue genome editing of *BCL11A* erythroid-specific enhancer for autologous cell therapy for SCD patients.

## RESULTS

### Upregulation of Fetal Globin Expression upon ZFN-Mediated Disruption of the *BCL11A* Gene

ZFNs targeting exon 2 (coding ZFNs) or the GATAA motif<sup>31,32</sup> within an intronic erythroid-specific enhancer (enhancer ZFNs) of the *BCL11A* gene<sup>33</sup> were engineered (Figure 1A). Introduction of ZFN mRNA via electroporation into BM-CD34<sup>+</sup> cells induced double-stranded DNA breaks that were repaired by the NHEJ DNA repair pathway. This produced a spectrum of small insertions or deletions (indels) centered at the targeted cleavage site, which was quantitated by targeted amplicon sequencing (Figures 1B and 1C). When primary BM-CD34<sup>+</sup> cells were transfected with escalating amounts of mRNAs encoding the ZFNs, increased levels of indels were detected until a plateau (~60% of total alleles) was reached (Figure 2A, left panel). When these transfected CD34<sup>+</sup> cells were further cultured under erythroid conditions, they gave rise to erythroid cells with corresponding increases in indels (Figure 2A, middle panel) and in their fetal globin expression, which reached as high as 35% of total  $\beta$ -like globin chains ( $G\gamma + A\gamma + \beta + \delta$ ) in both groups, as gauged by reverse phase high-performance liquid chromatography (HPLC) (Figure 2A, right panel).

The *BCL11A* knockout (KO) alleles, defined as having indels that caused frameshift mutations in exon 2 (Figure 1B) or disruption of the GATAA motif<sup>32</sup> in the erythroid-specific enhancer (Figure 1C), were quantitated. KO alleles were found to be less frequent at the population level after erythroid differentiation than in the starting pool of the treated BM-CD34<sup>+</sup> cells. This difference was more pronounced in samples treated with the coding ZFNs than those treated with the enhancer ZFNs (Figure 2B; Figure S1). These results suggest that frameshift mutations in the coding sequence of *BCL11A* may be counter-selected during erythroid differentiation.

### Effects of ZFN-Mediated Disruption of the *BCL11A* Gene on Terminal Erythroid Differentiation and Fetal Globin Induction at the Single Erythroid Progenitor Level

Because erythroid cells derived from bulk CD34<sup>+</sup> cell cultures originated from a pool of heterogeneous edited cells (Figure 1), they did not provide sufficient resolution to assess whether erythroid differentiation was affected by the editing and whether fetal globin was up-regulated to levels predicted to inhibit HbS polymerization. To address this issue, we sorted ZFN mRNA-treated BM-CD34<sup>+</sup> cells onto 96-well plates to allow for clonal derivation of mature erythroid

cells from individual burst-forming unit-erythroid (BFU-E) progenitors. When binned based on the genotype of each erythroid colony, it was revealed that by 17–18 days post erythroid culture, erythroid colonies with bi-allelic knockout (KO/KO) of exon 2 expressed predominantly fetal globin ( $G\gamma + A\gamma$ ), accounting for 80% of total  $\beta$ -like globin chains as measured by ultra-performance liquid chromatography (UPLC), with reciprocal reduction in adult  $\beta$ -globin (Figure 3A, left panel; Figures S2 and S3). The fetal globin levels expressed in KO/KO colonies were significantly higher than that in either WT/KO or WT/WT colonies ( $p < 0.0001$ ). However, the coding KO/KO erythroid progenitors gave rise to fewer erythroid cells than the WT/WT or WT/KO erythroid progenitors (two out of three donors) (Figure 3A, middle panel; Figure S2B, middle panel), which may have partially contributed to the aforementioned decrease in KO indel frequency after erythroid differentiation (Figure 2B; Figure S1). In addition, coding KO/KO colonies had significantly lower mean enucleation rates (three out of three donors) than colonies identified as WT/KO or WT/WT ( $p < 0.0001$ ) (Figure 3A, right panel; Figure S2B, right panel). This reduced enucleation efficiency was specific to coding KO/KO genotype, because cells with bi-allelic in-frame mutations enucleated as efficiently as unedited colonies (Figure S2C). Consistent with the flow-based enucleation assessment, cytopins of day-18 erythroid cells showed mostly enucleated RBCs in coding WT/WT and WT/KO colonies, but mostly nucleated erythroblasts in KO/KO colonies (Figure 4A, top row). The majority of erythroblasts, regardless of the genotype, resembled orthochromatic erythroblasts morphologically (Figure 4A) and expressed low levels of alpha 4 integrin and high levels of RhD blood group antigen, a hallmark of late erythroblasts<sup>34</sup> (Figure 4B). These data suggest that coding KO/KO erythroid progenitors were capable of progressing to the stage of orthochromatic erythroblasts but were less efficient in nuclear extrusion than their WT/WT or WT/KO counterparts.

When the impact of ZFN-mediated *BCL11A* erythroid enhancer GATAA motif disruption was assessed, increased levels of fetal globin expression, averaging 37% of total  $\beta$ -like globin chains based on data from five individual donors, were observed in GATAA motif KO/KO erythroid cells compared with GATAA motif WT/WT or WT/KO cells (Figure 3B, left panel; Figures S2 and S3). However, in contrast to the adverse effects of *BCL11A* exon 2 editing on enucleation, the GATAA motif KO/KO mutations did not impact enucleation efficiency (Figure 3B, right panel; Figure S2B). Cytopins confirmed the flow-based findings and showed that similar to GATAA motif WT/WT and WT/KO erythroid cells, GATAA motif KO/KO day-18 erythroid cells were mostly RBCs (Figure 4A, bottom row). The majority of the remaining erythroblasts had low alpha 4 integrin and high RhD blood group antigen expression and resembled orthochromatic erythroblasts regardless of their genotype (Figure 4B). These data indicate that the disruption of *BCL11A* erythroid-enhancer GATAA motif significantly increases fetal globin expression in terminally matured erythroid cells without interfering with the differentiation or maturation of erythroid progenitors.

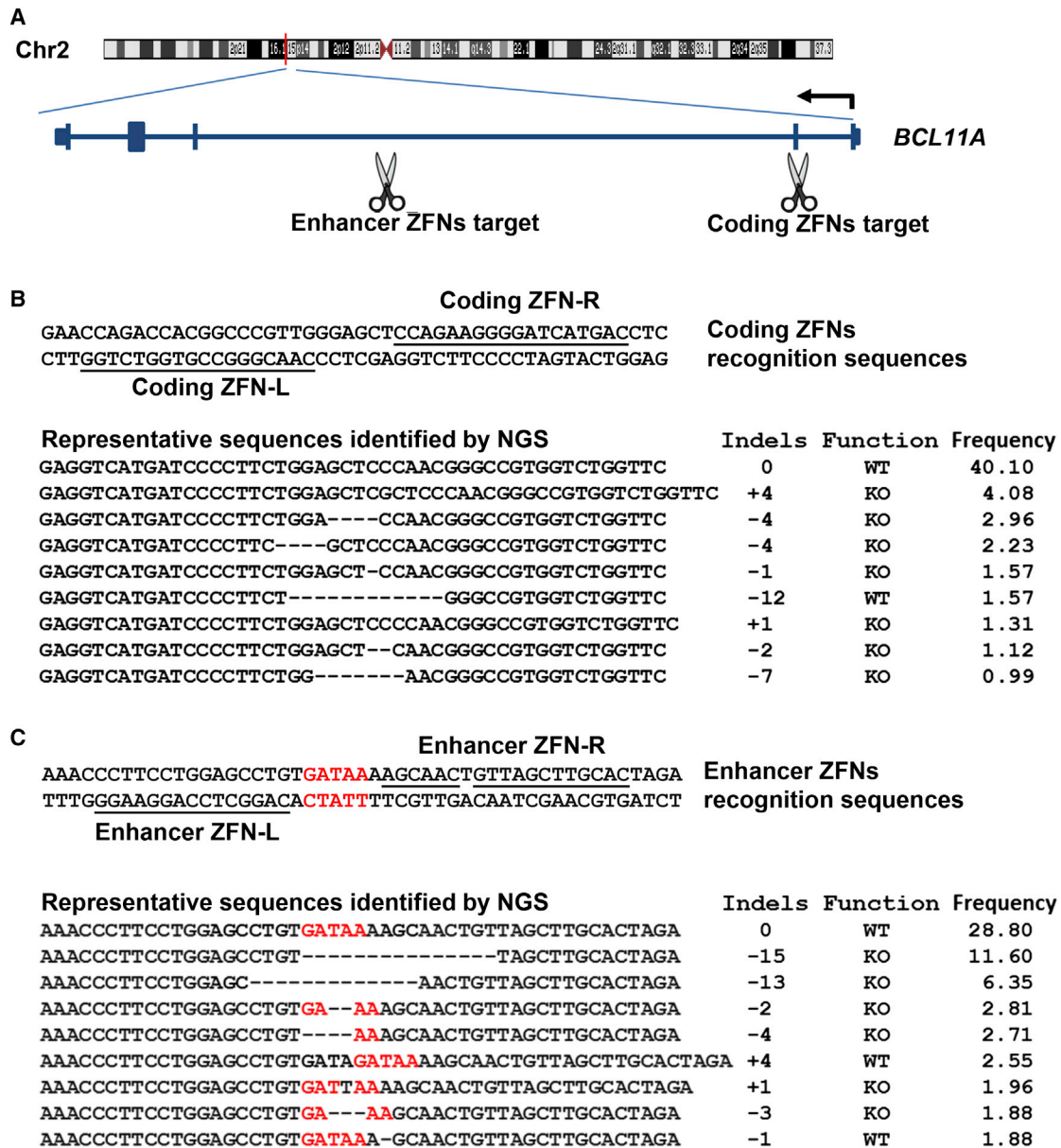


**Figure 1. Genome Editing of the *BCL11A* Gene by ZFNs**

(A) Schematic representation of the location within the *BCL11A* locus targeted by coding ZFNs or enhancer ZFNs. Coding ZFN-L, coding ZFN-R, and enhancer ZFN-R each has six fingers. Enhancer ZFN-L has five fingers. (B) Genomic sequences recognized by the coding ZFNs and representative sequences identified by next-generation deep sequencing (NGS) following ZFN treatment. Frameshift mutations are categorized as knockout (KO), whereas unedited alleles or in-frame mutations are categorized as wild-type (WT). Frequency refers to the percentage of sequencing reads identified as a specific sequence among total sequencing reads at this site. (C) Genomic sequences recognized by the enhancer ZFNs and representative sequences identified by NGS following ZFN treatment. Sequences with an intact GATAA motif are scored as WTs, whereas mutations that disrupt the GATAA motif are scored as KOs.

***BCL11A* Exon 2 Editing Impairs Engraftment of BM-CD34<sup>+</sup> Cells**

To determine the engraftment potential of genome-edited HSPCs, we transplanted ZFN-treated BM-CD34<sup>+</sup> cells into NOD/SCID/IL2rg null (NSG) mice (Figure 5). Repopulated human cells (hCD45<sup>+</sup>) were readily detectable in the peripheral blood (PB) of all transplanted

animals at week 8 post-transplant (Figure 5A). However, a sharp decline in indel frequency post-transplant was observed in the coding ZFN-treated group, but much less so in the enhancer ZFN-treated group (Figure 5B), despite that the CD34<sup>+</sup> cell viabilities were comparable after electroporation at the time of harvesting (Table S1). This is

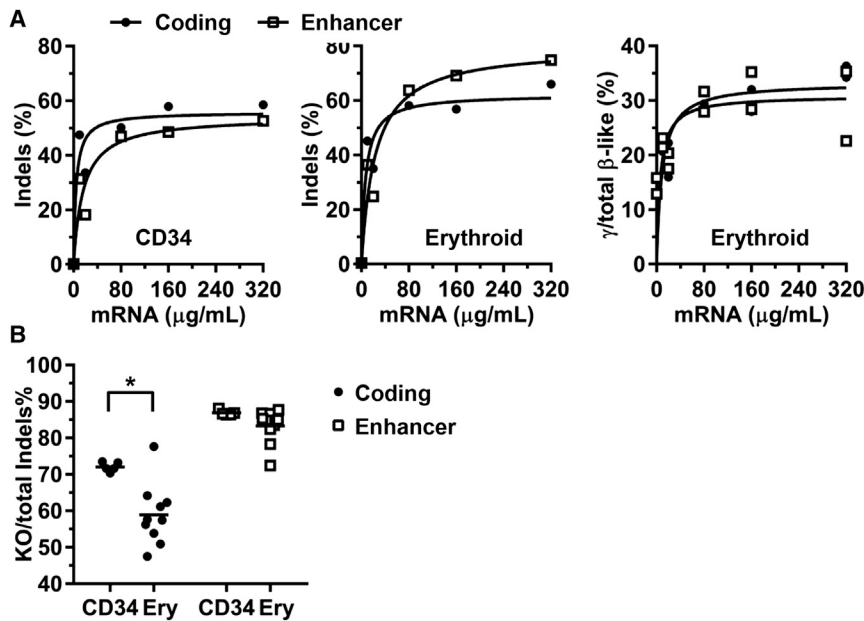


**Figure 2. In Vitro Analysis of BM-CD34<sup>+</sup> Cells Treated with mRNAs Encoding ZFNs at the Population Level**

(A) BM-CD34<sup>+</sup> cells were transfected with indicated amounts of the ZFN mRNAs targeting either the exon 2 (coding ZFNs) or the GATAA motif in the erythroid-specific enhancer (enhancer ZFNs) of the *BCL11A* gene using a BTX electroporator. Indels were determined by deep sequencing 72 hr after CD34<sup>+</sup> cell transfection (left panel) or 14 days after erythroid differentiation of edited CD34<sup>+</sup> cells (middle panel). Fetal globin expression by day-17 erythroid cells was determined by reverse phase HPLC and expressed as  $(G\gamma+A\gamma)/(G\gamma+A\gamma+\delta+\beta)$  (%) (right panel). (B) Percentages of indels in CD34<sup>+</sup> cells or in erythroid progeny (Ery) that resulted in either frameshift mutations in the coding ZFN-treated samples or disruption of the GATAA motif in the enhancer ZFN-treated samples. Data are pooled from all treatment groups presented in (A). Each dot represents one sample. Mean values for groups in (B) are shown. \* $p < 0.05$ .

consistent with the recently described role of *BCL11A* in maintaining HSC functions.<sup>22,35,36</sup> Taken together, the negative impact of exon 2 disruption of the *BCL11A* gene on both terminal erythroid enucleation as well as on HSC function strongly argues against disruption of the coding sequence of *BCL11A* as a therapeutic strategy.

#### ***BCL11A* Enhancer-Edited BM-CD34<sup>+</sup> Cells Support Long-Term Engraftment and Fetal Globin Reactivation**

In order to more thoroughly examine the impact of *BCL11A* enhancer ZFN treatment, we performed additional long-term engraftment studies of enhancer ZFN-edited BM-CD34<sup>+</sup> cells (Figure 6). Human chimerism in circulation was similar between control and enhancer ZFN-treated groups for at least 16 weeks (Figure 6A). Examination of the chimeric BM showed that the engraftment was multilineage. CD19<sup>+</sup> B cell lineage was the primary human cell type in BM, followed by CD33<sup>+</sup> myeloid lineage. Low levels of CD3<sup>+</sup> T cells, CD56<sup>+</sup> NK cells, and CD34<sup>+</sup> HSPCs were also detected. Human chimerism levels in BM were largely indistinguishable between control and enhancer ZFN-treated groups except for minor but statistically significant differences in CD19<sup>+</sup> and CD33<sup>+</sup> populations. Importantly, indels within the *BCL11A* enhancer were maintained at approximately 45%–50% in PB (Figure 6B), reproducing the data reported in Figure 5. In addition, similar indel retention was observed in total BM, individually sorted CD3<sup>+</sup>, CD19<sup>+</sup>, and CD33<sup>+</sup> cell populations, as well as in human granulocytes or macrophages (GM), and erythroid cells differentiated ex vivo from the chimeric BM of primary recipients at 16 weeks post-transplant (Figure 6B). The high levels of indels in ex-vivo-derived erythroid cells from the enhancer ZFN-treated group coincided with an increased percentage of erythroid cells expressing fetal globin (F cells) and elevated overall fetal globin levels compared with cells from the control group, whereas comparable levels of enucleation were attained (Figure 6C).

Because any human BFU-E erythroid progenitors present in chimeric BM at 16 weeks post-transplant were likely derived from engrafted long-term HSCs, it was estimated that roughly 26% of the long-term engrafting HSCs from the input BM-CD34<sup>+</sup> cells were GATAA motif KO/KO and 14% were GATAA motif WT/KO (Figure 6D).

Finally, the BM cells of primary recipient mice at 16 weeks post-transplant were injected into secondary recipients. Low, yet comparable levels of human chimerism was achieved in control versus enhancer ZFN-treated groups at 8 weeks post-secondary transplant (Figure 6E). Approximately 23% of the human *BCL11A* alleles bore indels (Figure 6F). These data provide strong evidence that the *BCL11A* erythroid enhancer in human long-term engrafting HSCs can be edited by ZFNs.

#### **DISCUSSION**

Fetal hemoglobin (HbF,  $\alpha_2\gamma_2$ ) is recognized as one of the most important disease modifiers for SCD because it not only inhibits HbS polymerization, but also reduces mean corpuscular HbS concentration.<sup>5,37–40</sup> HbF is the predominant hemoglobin at birth, but it typically falls below 1% of total hemoglobin within a year and is replaced by adult hemoglobin ( $\alpha_2\beta_2$ ) as the switch from  $\gamma$ - to  $\beta$ -globin in the  $\beta$ -globin locus occurs.<sup>4</sup> Pharmacologic reactivation of HbF presents one strategy to treat SCD and has received tremendous attention in the field. Conceptually it is also possible to permanently reactivate fetal globin expression by interfering with the fetal globin silencing machinery via genomic manipulation of a patient's autologous HSCs. The  $\beta$ -globin locus itself, *BCL11A*, and the *HBS1L-MYB* intergenic region have been associated with hereditary persistence of fetal hemoglobin (HPFH) in genome-wide association studies (GWAS)<sup>19,41–43</sup> and provide tangible molecular targets for such an approach. Indeed, two recent studies have utilized

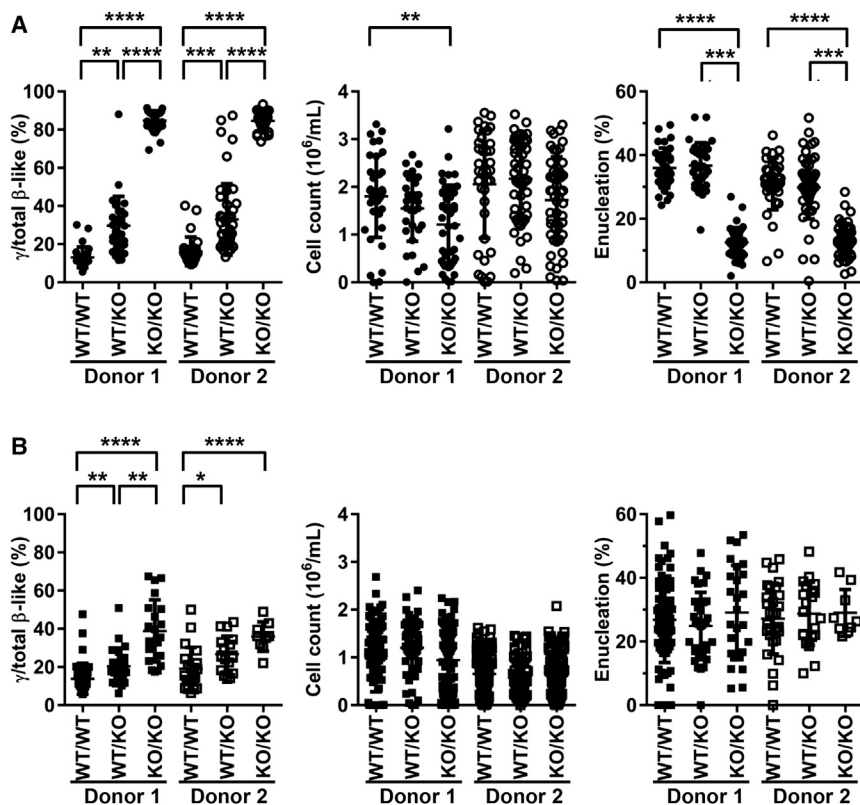


**Figure 3. In Vitro Analysis of Clonally Derived Erythroid Cells from BM-CD34<sup>+</sup> Cells Treated with mRNA-Encoding ZFNs**

(A) BM-CD34<sup>+</sup> cells were transfected with mRNA encoding the coding ZFNs at 100  $\mu$ g/mL using a BTX electroporator and sorted onto 96-well plates at two cells per well and cultured under erythroid conditions. Clonally derived erythroid cells grown from CD34<sup>+</sup> cells treated with the coding ZFNs were analyzed for fetal globin expression by UPLC (left panel) and cell number (middle panel) and enucleation (right panel) by flow cytometry. Data are grouped based on the genotype of the erythroid clones, as determined by deep sequencing. KOs refer to frameshift mutations, and WTs include unedited alleles and in-frame mutations. (B) Same as (A) except that CD34<sup>+</sup> cells were treated with enhancer ZFNs mRNA at 100  $\mu$ g/mL. KOs refer to indels that disrupt the GATAA motif in the erythroid enhancer and WTs include unedited alleles and indels that do not disrupt the GATAA motif. Although CD34<sup>+</sup> cells from the same donors were used, transfections with coding ZFNs or enhancer ZFNs were performed on different dates. Each dot represents one sample. Mean  $\pm$  SD for each group is shown. \* $p < 0.05$ , \*\* $p < 0.01$ , \*\*\* $p < 0.001$ , \*\*\*\* $p < 0.0001$ .

CRISPR-Cas9-mediated genome editing to recapitulate known HPFH mutations in the  $\beta$ -globin locus in the primary human CD34<sup>+</sup> cells.<sup>44,45</sup> Although upregulated fetal globin expression in the erythroid progeny of CD34<sup>+</sup> cells is observed, it remains to be seen at what frequency long-term repopulating HSCs have been targeted by these genome-editing strategies.

In this study, we used the ZFN genome-editing technology to target *BCL11A* in primary human BM-derived CD34<sup>+</sup> cells instead of mobilized PB-derived CD34<sup>+</sup> cells<sup>46</sup> because of the potentially life-threatening complications when mobilizing SCD patients with granulocyte colony-stimulating factor (G-CSF).<sup>47</sup> *BCL11A* is a key suppressor of fetal globin expression,<sup>17,18,20,48</sup> and the conditional knockout of *BCL11A* in the erythroid lineage significantly increases fetal globin expression and cured a mouse model of SCD.<sup>30</sup> Here, two targeting strategies were employed. The first strategy targeted exon 2 of the *BCL11A* gene. Because exon 2 is shared by all *BCL11A* isoforms, frameshift mutations in this region should completely inactivate *BCL11A* expression from the edited alleles. Although Bjurstrom and colleagues<sup>46</sup> show that *BCL11A* exon 2-edited mobilized PB-CD34<sup>+</sup> can successfully engraft NSG mice, we found the engraftment by edited BM-CD34<sup>+</sup> cells to be severely impaired (Figure 6). Because it has recently been reported that *BCL11A* not only is important for lymphoid development,<sup>49</sup> but also plays a critical role in maintaining vital HSC functions,<sup>22,35,36</sup> a defect in the engraftment of exon 2 KO/KO cells was therefore not unexpected. In contrast to being essential

for preserving HSC functions, it has been reported that *BCL11A* is dispensable for RBC production based on data obtained from erythroid-specific knockout of *BCL11A* in mice and shRNA knockdown of *BCL11A* in primary human erythroblasts.<sup>22,30</sup> Although we found that *BCL11A* coding KO/KO erythroid progenitors were capable of differentiating and maturing into orthochromatic erythroblasts, the enucleation efficiency of coding KO/KO erythroid cells was significantly lower than their WT/WT or WT/KO counterparts (Figures 3 and 4; Figure S2). The reason behind the suboptimal enucleation in coding KO/KO cells is not clear. However, this is unlikely an outcome of potential off-target editing because impaired enucleation was observed only in cells with bi-allelic out-of-frame mutations, and not in those with bi-allelic in-frame mutations at *BCL11A* exon 2. In any case, suboptimal engraftment of exon 2-edited CD34<sup>+</sup> cells and reduced erythroid enucleation suggest that genome editing of the coding region of *BCL11A* is not a sustainable strategy for SCD.

As an alternative, we targeted an erythroid-specific enhancer within the second intron of the *BCL11A* gene that controls *BCL11A* expression exclusively within that cell lineage.<sup>33</sup> More specifically, ZFNs were engineered to target the GATAA motif, a key regulatory element situated in the +58 DNaseI hypersensitive site of the enhancer.<sup>31–33</sup> Unlike *BCL11A* exon 2 editing, bi-allelic knockout of the GATAA motif did not affect enucleation efficiency (Figures 3 and 4; Figure S2), presumably because of residual *BCL11A* expression.<sup>22,31</sup> Although the induction of fetal globin expression in enhancer KO/KO erythroid cells was less robust than that in coding KO/KO erythroid cells, the levels of fetal globin expression, averaging 37% of total  $\beta$ -like globins

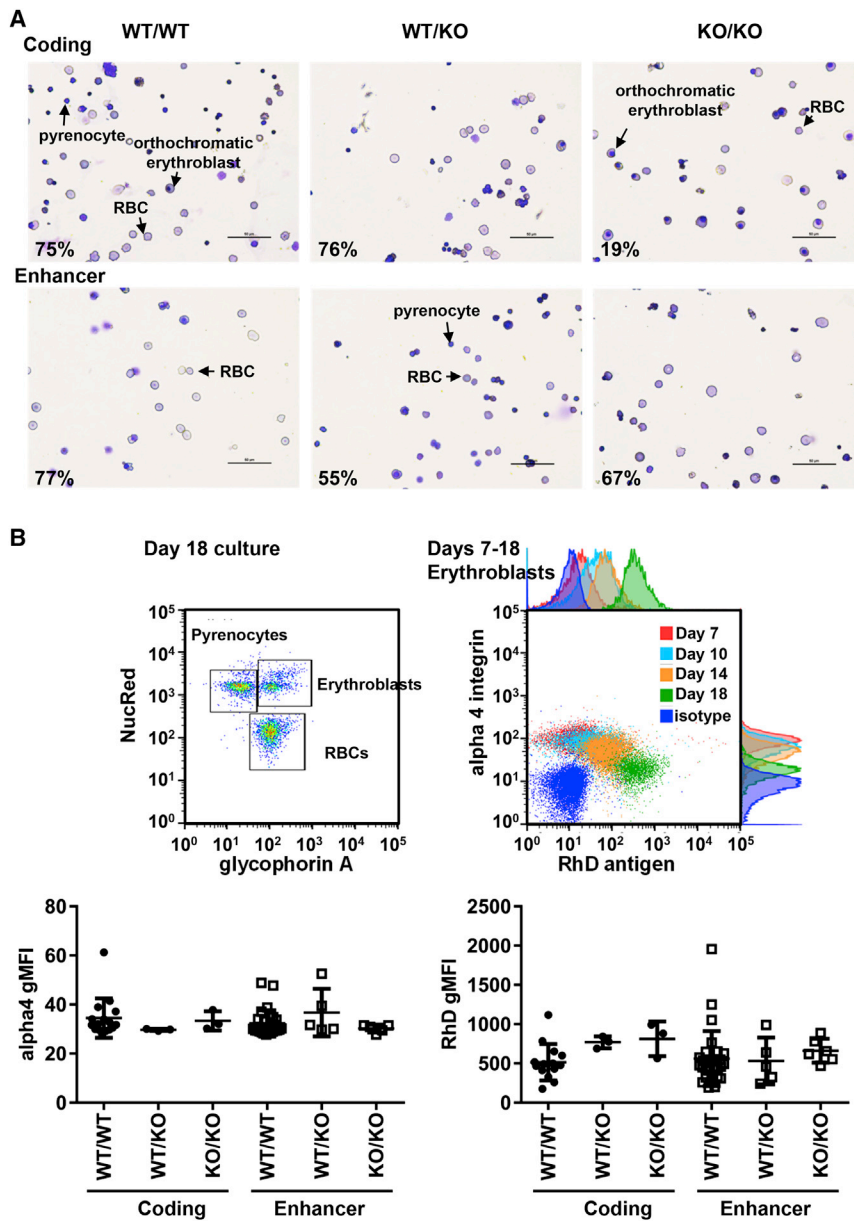


**Figure 4. Phenotypic and Morphological Examination of Day-18 Erythroid Cultures Derived from Single BM-CD34<sup>+</sup> Cells Treated with mRNA-Encoding ZFNs**

(A) BM-CD34<sup>+</sup> cells were transfected with mRNA encoding either coding ZFNs or enhancer ZFNs at 300  $\mu$ g/mL using a MaxCyte electroporator. They were sorted onto 96-well plates and cultured under erythroid conditions. Cytospins were made from day-18 cultures. Representative pictures are shown. Pyrenocytes, RBCs, and late erythroblasts can be clearly seen with all genotypes. The images were acquired using a Nikon eclipse Ci microscope with a Nikon Plan 40X/0.65 objective lens, a Nikon DS-F12 camera, and NIS-Elements D imaging software version 4.30.01 (Nikon). The numbers shown on the lower left-hand corners indicate the RBC frequency in each culture. Scale bars, 50  $\mu$ m. (B) Day-18 erythroid cells were stained for glycoprotein A, alpha 4 integrin, RhD antigen, and nucleus. Cells can be identified as pyrenocytes, erythroblasts, and RBCs based on glycoprotein A and nuclear staining<sup>64</sup> (top left panel). The kinetic changes of alpha 4 integrin and RhD blood antigen<sup>64</sup> expression by erythroblasts at various time points during a bulk erythroid culture are provided as a reference (top right panel). The expression levels of alpha 4 integrin (bottom left) and RhD antigen (bottom right), presented as geometric mean fluorescence intensity (gMFI), of day-18 erythroblasts were analyzed. Data are grouped based on the genotype of the colonies. Mean  $\pm$  SD for each group is shown. No statistically significant differences were found.

at levels similar to those detected in patients with *BCL11A* haploinsufficiency,<sup>51,52</sup> which validates the relevancy of our in vitro system.

Finally, in contrast to *BCL11A* exon 2 editing, the enhancer-edited BM-CD34<sup>+</sup> cells achieved robust, long-term engraftment in NSG mice. Genotyping of BFU-E colonies derived from the repopulated human cells in chimeric BM provided much-needed quantification of the editing efficiency in long-term repopulating HSCs, which could only be assayed in NSG mice or similar in vivo model systems. Based on allogeneic HSCT data,<sup>53,54</sup> mouse studies,<sup>55,56</sup> and mathematical modeling,<sup>57,58</sup> non-S HSC chimerism as low as 10%–20% may lead to clinical improvement. If gene-edited, high fetal globin-expressing SCD RBCs have a similar survival advantage as normal RBCs, a frequency of 26% GATAA motif KO/KO HSCs and 14% WT/KO HSCs should offer long-term, substantial alleviation of symptoms in SCD patients.

Altogether, our data provide in vitro and in vivo evidence that the GATAA motif in the erythroid-specific enhancer of *BCL11A* gene is an effective and safe target compared with the *BCL11A* coding region for gene disruption for the treatment of SCD. ZFN-mediated

with a reciprocal reduction in adult  $\beta$ -globin, should nevertheless be sufficient to inhibit HbS polymerization if maintained in vivo.<sup>4,50</sup> It should be noted that the quantification of fetal globin protein expression was done within clonally derived erythroid cells. This is particularly important because fetal globin expression at the individual cell level, and not at the population level, determines whether the erythrocytes can be protected from HbS polymerization.<sup>4</sup> Furthermore, the enhancer WT/KO erythroid cells had a moderate increase of fetal globin expression, which can also be disease-modifying given the inverse relationship between fetal globin level and SCD mortality.<sup>11</sup> It is also noteworthy that mono-allelic GATAA motif KO erythroid cells, as well as mono-allelic exon 2 KO erythroid cells, expressed fetal globin

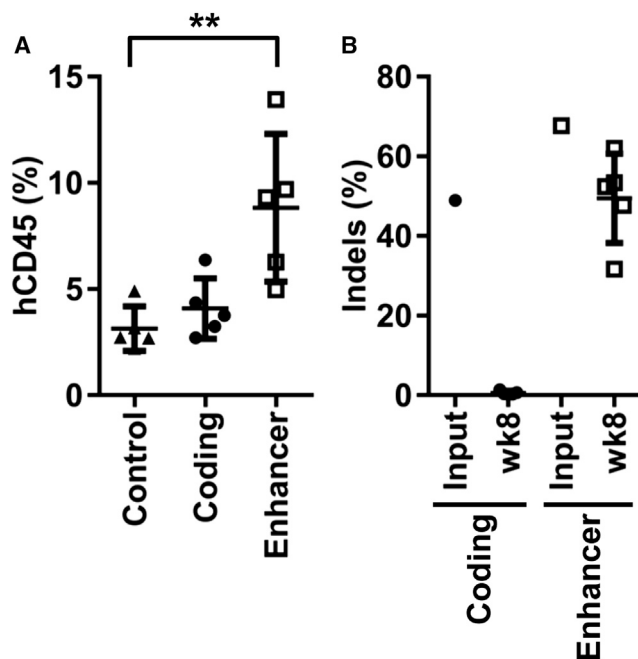


**Figure 5. Xenotransplantation of BM-CD34<sup>+</sup> Cells Edited with Either *BCL11A* Coding or Enhancer ZFNs**

(A) BM-CD34<sup>+</sup> cells were treated with mRNA encoding either the coding ZFNs or the enhancer ZFNs at 300 μg/mL using a MaxCyte electroporator and transplanted into NSG mice. Untreated cells were transplanted as controls. PB was sampled at week 8 after transplantation and analyzed for human chimerism by flow cytometry. (B) Indels within the human *BCL11A* gene were determined by deep sequencing at week 8 post-transplant. Each dot represents one mouse, and mean ± SD for each group is shown. \*\*p < 0.01.

editing of this GATAA motif occurs efficiently in functional long-term repopulating HSCs and does not interfere with terminal erythroid maturation. Furthermore, GATAA-motif disruption produces erythroid cells that express fetal globin at levels predicted to be effective in inhibiting HbS polymerization. Therefore, our results provide a strong preclinical proof-of-concept that supports the clinical development of genome editing to disrupt the *BCL11A* erythroid-specific enhancer in autologous HSCs as a potentially curative therapy for SCD patients.

## MATERIALS AND METHODS

### *BCL11A* Editing of BM-CD34<sup>+</sup> Cells Using ZFNs

ZFNs that target either the exon 2 (coding ZFNs) or the GATAA motif in an erythroid-specific enhancer (enhancer ZFNs) of the *BCL11A* gene<sup>31–33</sup> (Figure 1) were engineered by Sangamo BioSciences as previously described.<sup>32</sup> BM-CD34<sup>+</sup> cells were isolated from de-identified BM aspirates of healthy volunteers (Hemacare). Briefly, de-identified BM aspirates from multiple ABO-matched donors were pooled, RBC-depleted with hetastarch,<sup>59</sup> and then enriched with the CliniMACS Prodigy using CliniMACS CD34 microbeads per the manufacturer's instructions (Miltenyi Biotec). Enriched BM-CD34<sup>+</sup> cells were cryopreserved in Cryostor CS10 (Sigma-Aldrich) using a controlled rate freezer and stored in the vapor phase of a liquid

nitrogen Dewar. Alternatively, cryopreserved BM-CD34<sup>+</sup> cells were purchased from Lonza (Hopkinton, MA), STEMCELL Technologies, or Hemacare. To edit BM-CD34<sup>+</sup> cells, we thawed and cultured cryopreserved cells in CD34 maintenance media, comprised of X-VIVO-10 (Lonza), 1X GlutaMAX, 100 U/mL penicillin, 100 μg/mL streptomycin (all three from Thermo Fisher Scientific), and recombinant human thrombopoietin (TPO), FMS-like tyrosine kinase 3 ligand (FLT3L), and stem cell factor (SCF) (100 ng/mL each; PeproTech) for 1 or 2 days<sup>25</sup> at 37°C, 5% CO<sub>2</sub> in a humidified incubator. Electroporation of ZFN mRNA was performed either with a BTX ECM 830 Square Wave Electroporator (Harvard Apparatus) or a MaxCyte device per the manufacturer's instructions. After transfection, cells were incubated in the CD34 maintenance media at 30°C for 16 hr and then at 37°C for 24 hr. The treated BM-CD34<sup>+</sup> cells were either analyzed directly or cryopreserved.

### In Vitro Erythroid Differentiation

CD34<sup>+</sup> cells were differentiated into erythroid cells using a three-step differentiation protocol developed by Luc Douay's group.<sup>60</sup> In brief, CD34<sup>+</sup> cells were cultured for 7 days in Step-1 media consisting of Iscove's modified Dulbecco's medium (IMDM) (Thermo Fisher Scientific) supplemented with 1X GlutaMAX, 100 U/mL penicillin, 100 μg/mL streptomycin, 5% human AB<sup>+</sup> plasma, 330 μg human holo-transferrin, 20 μg/mL human insulin, 2 U/mL heparin, 1 μM hydrocortisone (all four from Sigma-Aldrich), 3 U/mL recombinant human erythropoietin (EPO) (Thermo Fisher Scientific), 100 ng/mL SCF, and 5 ng/mL interleukin-3 (IL-3) (all three from PeproTech). On day 7, cells were transferred to Step-2 media, which was identical to step 1 media except the absence of hydrocortisone and IL-3, and cultured for 3–4 days. Next, cells were cultured for 7–9 days in step 3 media, which was similar to step 2 media but without the addition of SCF.

To determine the enucleation rate, we stained cells with NucRed (Thermo Fisher Scientific) per the manufacturer's instruction. Cells were acquired using a FACSCanto, and analysis was done using FlowJo software V10 (Tree Star).

To determine the percentage of HbF-positive cells, cells were fixed with 4% formaldehyde (Sigma-Aldrich), permeabilized with ice-cold acetone (Thermo Fisher Scientific), washed with PBS (Thermo Fisher Scientific) supplemented with 0.5% BSA (Sigma-Aldrich), and stained with fluorescein isothiocyanate (FITC)-conjugated anti-γ-globin antibody (Santa Cruz) according to the method by Thorpe et al.<sup>61</sup>

Globin chain expression was measured by UPLC or HPLC, modified from a published protocol.<sup>62</sup> For UPLC, 5 μL of hemolysate was injected onto a Waters Acquity UPLC Protein BEH C4 Column (300A, 1.7 micron, 2.1 × 100 mm). Elution was obtained at room temperature with a flow rate of 0.2 mL/min using an 18-min linear gradient of 38%–42.5% acetonitrile in water (both from Thermo Fisher Scientific). Trifluoroacetic acid was added to both water and acetonitrile to maintain a constant concentration of 0.1%. Elution was followed at 220 nm with no reference wavelength and

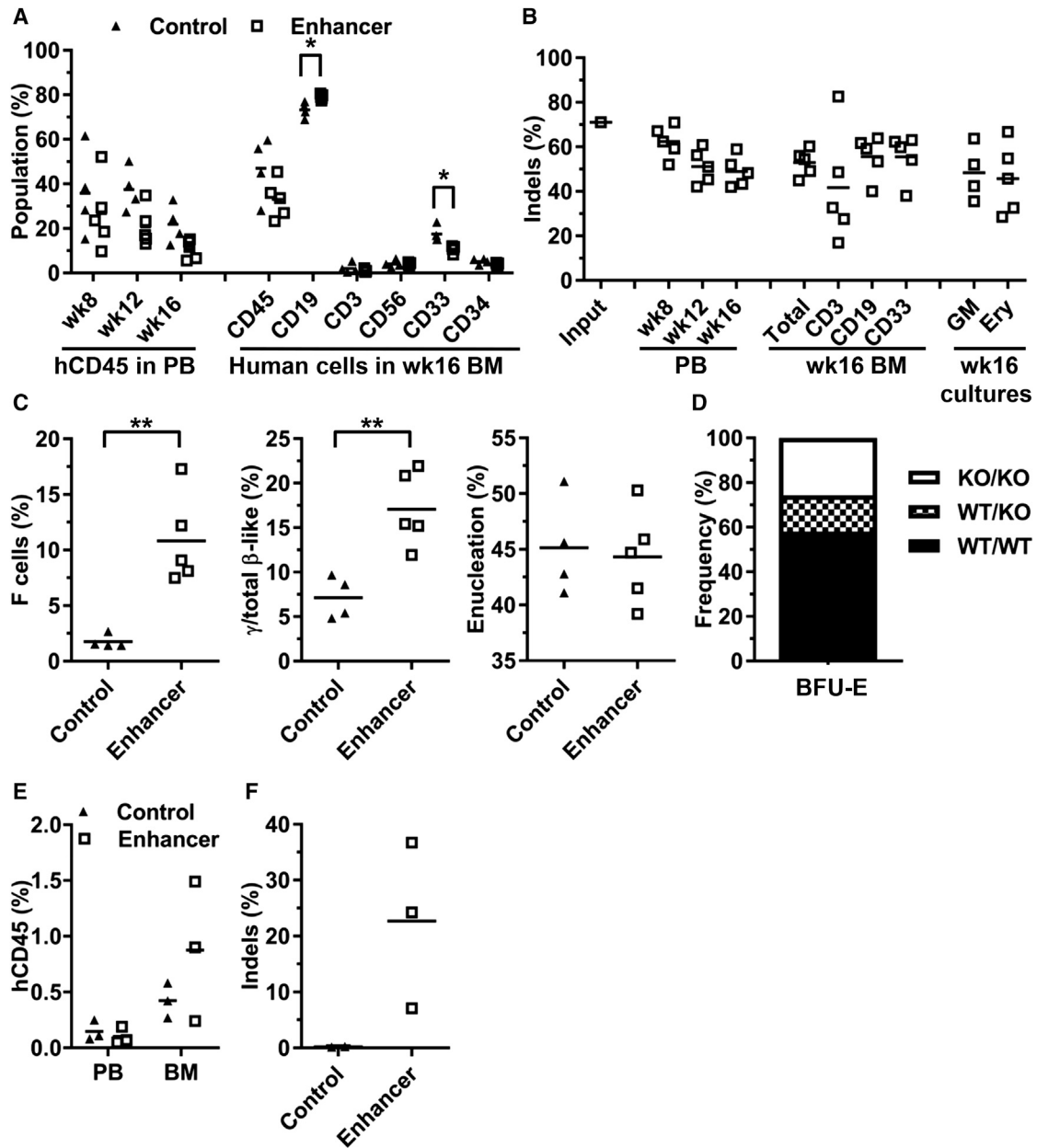


**Figure 6. Engraftment Analysis of BCL11A Enhancer-Edited BM-CD34<sup>+</sup> Cells in NSG Mice**

(A) BM-CD34<sup>+</sup> cells were treated with mRNA encoding the enhancer ZFNs at 300  $\mu$ g/mL using a MaxCyte electroporator and transplanted into NSG mice. Untreated cells were transplanted as controls. PB and BM from primary recipients were sampled at indicated times and analyzed by flow cytometry for human chimerism (hCD45) in PB and BM, as well as for multilineage reconstitution in BM, expressed as a percentage of hCD45<sup>+</sup> cells. (B) Indels within the human *BCL11A* gene in PB, BM, various human hematopoietic lineages sorted from BM, and granulocytes or macrophages (GM) and erythroid cells (Ery) differentiated ex vivo from the BM of the engrafted mice were quantified by deep sequencing. (C) Erythroid cells differentiated from the chimeric BM at week 16 of the primary recipients were evaluated for fetal globin expression by flow cytometry (left panel) and by UPLC (middle panel), as well as for enucleation by flow cytometry (right panel). (D) BM cells from primary recipients at week 16 post-transplant were plated in MethoCult methylcellulose media, and 173 BFU-E colonies were plucked and genotyped. The targeted loci with an intact GATAA motif were scored as WTs, and mutations that disrupted the GATAA motif were scored as KOs. (E) BM cells from five primary recipients of the same treatment group at week 16 post-transplant were pooled, depleted for B220<sup>+</sup>, TER119<sup>+</sup>, and mouse CD117<sup>+</sup> cells, and then injected via tail vein into three irradiated recipients. Human chimerism in PB and BM of secondary recipients at 8 weeks post-transplant was determined. (F) Indels within human *BCL11A* gene in BM of secondary recipients at 8 weeks post-transplant. (A–C, E, and F) Each dot represents one mouse. Mean for each group is shown. \* $p < 0.05$ , \*\* $p < 0.01$ .



**Table 1. Primers Used for Deep Sequencing**

Name	Sequence (5' to 3')
BCL11A coding F	TCGTCGGCAGCGTCAGATGTGTATAAGAGACAGTCTAAGCAGAGGCTGCCATT
BCL11A coding R	GTCTCGTGGGCTCGGAGATGTGTATAAGAGACAGATGGGGTTGAGATGTGCTTC
BCL11A enhancer F	TCGTCGGCAGCGTCAGATGTGTATAAGAGACAGCCAGTGCAAAGTCCATACAGG
BCL11A enhancer R	GTCTCGTGGGCTCGGAGATGTGTATAAGAGACAGGCTGCCAGTCTCTTCTACC

280 nm with reference at 360 nm. Area percentage for specific globin chains: A $\gamma$ , G $\gamma$ ,  $\beta$ ,  $\delta$ , or  $\alpha$ , representing the relative amount of each specific globin chain, was quantitated using Agilent OpenLAB software. For HPLC, 20  $\mu$ L of hemolysate was injected onto a Grace Vydac C4 Column (5 micron, 4.6  $\times$  250 mm). Elution was obtained at room temperature with a flow rate of 1 mL/min using a 30-min linear gradient of 38.4%–43.8% acetonitrile in water with trifluoroacetic acid constant at 0.1%. Area percentage for specific globin chains was determined at 220 nm using Agilent Chemstration software.

#### Single-Cell Clonal Expansion Analysis

For single-cell studies, transfected CD34<sup>+</sup> cells were sorted into step 1 erythroid culture media (200  $\mu$ L/well) in 96-well U-bottom non-TC-treated plates (Corning) at two cells/well using FACSaria III because a pilot experiment showed that less than 20% of the CD34<sup>+</sup> cells gave rise to erythroid colonies. After 7 days of culture, 150  $\mu$ L of media per well was removed and replaced with 100  $\mu$ L step 2 erythroid culture media. After 4 additional days of culture, 100  $\mu$ L media per well was removed and replaced with 100  $\mu$ L step 3 media. On day 14 post-differentiation, 10  $\mu$ L of cell suspension per well was harvested for deep sequencing. Furthermore, 100  $\mu$ L of media per well was removed and replaced with 100  $\mu$ L of fresh step 3 media. Remaining cells were cultured for 3–4 more days when 50  $\mu$ L of cell suspension per well was collected, stained with an equal volume of NucRed (2 drops/mL in PBS with 0.5% BSA), and analyzed with Guava easyCyte for cell count and enucleation rate. Remaining cells were spun down, washed once with PBS, and lysed in 20  $\mu$ L HPLC-grade water. Cell debris was removed by centrifugation (10,000  $\times$  g, 15 min, 4°C). Hemolysate was stored at –80°C until ready for globin chain analysis by UPLC as described above.

For cell morphology examination, day-18 cultures were spun onto glass slides (Thermo Fisher Scientific) using a Shandon 4 Cytospin (Thermo Fisher Scientific) and stained with PROTOCOL Hema 3 Fixative and Solution (Thermo Fisher Scientific) per the manufacturer's instructions.

To characterize surface marker expression by erythroid colonies, we harvested day-18 erythroid cells and stained them with antibodies against glycophorin A<sup>63,64</sup> (catalog no. F0870; Dako, Agilent Pathology Solutions), alpha 4 integrin (category no. 563458; BD Biosciences) and RhD blood group antigen (catalog no. 130-104-819; Miltenyi Biotec). Cells were acquired using a Guava easyCyte (EMD Millipore). Analysis was done using FlowJo software.

#### Genotyping the Targeted Loci by Deep Sequencing

Disruption of targeted loci was quantitated by deep sequencing. In brief, genomic DNA was subjected to targeted PCR amplification using human *BCL11A*-specific primers that also bear sample-specific barcodes and the Illumina flow cell-specific sequences (P5 and P7) (Table 1). Libraries were sequenced for 150X2 paired-end reads on the MiSeq Sequencing System (Illumina) following the manufacturer's instructions.

After the MiSeq run, the forward and reverse paired-end reads were merged using paired-end read merger (PEAR).<sup>65</sup> The merged fragments were then clustered with exact forward and reverse primers. The primers and several following bases were trimmed off to eliminate sequencing and PCR errors in the beginning of a read. Next, fragments with the same length and high similarity were merged to further eliminate sequencing or PCR errors. To identify the mutations in the fragments, we compared reads that passed the above filters with the reference amplicon sequence via single-gap alignment.

#### Engraftment and Ex Vivo Differentiation

Female NOD.Cg-Prkdcscid IL2rgtm1Wjl/SzJ (NSG) mice (Jackson Laboratories) at the age of 6–7 weeks were sub-lethally irradiated at 300 rad 1 day before transplant. For primary recipients, human BM-CD34<sup>+</sup> cells were injected into the mice via the tail vein at approximately 1 million viable cells per mouse. Human chimerism in PB was evaluated by flow cytometry at weeks 8, 12, and 16 post-transplant. Mouse PB was sampled from the submandibular vein with EDTA as the anti-coagulant agent. RBCs were lysed using ACK lysing buffer (Thermo Fisher Scientific), and cells were washed with PBS supplemented with 0.5% BSA. A fraction of washed cells was spun down and stored at –20°C for DNA extraction and deep sequencing. For flow cytometry, washed cells were first incubated with Fc blocking antibodies (catalog no. 422302 and 101320; BioLegend) for 15 min, followed by the incubation with hCD45-allophycocyanin (APC)-Cy7 antibody (catalog no. 304014; BioLegend) and mCD45-BUV395 antibody (catalog no. 564279; BD Biosciences). The percentage human chimerism in PB was defined as %hCD45+/(%hCD45+%mCD45).

Primary recipients were euthanized at week 16 post-transplant. BM cells were collected from femurs, tibias, and pelvic bones for cell sorting, flow cytometry, ex vivo cultures, burst-forming unit-erythroid (BFU-E) cultures, and secondary transplant. Cell sorting was performed using a FACSaria III instrument (BD Biosciences). RBCs, debris, and doublets were first excluded by forward and side scatters.

Human CD45<sup>+</sup> cells were identified as positive by staining with the hCD45-BV510 antibody (catalog no. 563204; BD Biosciences). Specific lineages such as B cell (CD19), T cell (CD3), and myeloid precursors (CD33) within the hCD45<sup>+</sup> population were identified by the corresponding fluorochrome-conjugated human specific antibodies (CD19-R-phycoerythrin [PE], catalog no. 340364; CD3-FITC, catalog no. 561807; CD33-PE-CF594, catalog no. 562492; all from BD Biosciences) and sorted. The sorted cells were spun down and stored at -20°C for deep sequencing analysis. Lineage reconstitution in BM was determined by flow cytometry. Cells were acquired using the BD LSRII and analyzed with FlowJo. Antibodies used were hCD45-BV510 (catalog no. 563204), CD19-PE (catalog no. 555413), CD3-FITC (catalog no. 551378), CD33-PE-CF594 (catalog no. 562492), CD34-PE-Cy7 (catalog no. 560710) (all from BD Biosciences), and CD56-APC (catalog no. 318310; BioLegend). Erythroid differentiation was performed as described above. Granulocyte-monocyte/macrophage cell differentiation was performed by culturing BM cells in IMDM supplemented with 1X GlutaMAX, 100 U/mL penicillin, 100 µg/mL streptomycin, 5% human AB<sup>+</sup> plasma, 2 U/mL heparin, 50 ng/mL SCF, 5 ng/mL IL-3, 10 ng/mL granulocyte macrophage colony-stimulating factor (GM-CSF), and 20 ng/mL G-CSF (all recombinant human cytokines were purchased from PeproTech) for 14 days. For BFU-E cultures, BM cells were plated in semi-solid methylcellulose culture media supplemented with human growth factors (Methocult H4434; STEMCELL Technologies). Individual hemoglobinized erythroid colonies were genotyped 14 days after culture.

For secondary transplant, the remaining BM cells from five primary recipients were pooled, enriched for the repopulated human cells by depleting B220<sup>+</sup> cells, TER119<sup>+</sup> cells, and mouse CD117<sup>+</sup> cells, and then injected via tail vein into three irradiated recipients. Secondary recipients were euthanized 8 weeks post-transplant. PB and BM were harvested for human chimerism determination and deep sequencing as described above.

All procedures were performed in accordance with protocols approved by the Biogen Institutional Animal Care and Use Committee (IACUC).

### Statistical Analyses

Statistical differences between two samples were tested by the Mann-Whitney test. Multiple samples were statistically compared by the Kruskal-Wallis test followed by the Dunn's multiple comparisons test. The p values less than 0.05 were considered to be significant. Statistical analyses were performed using GraphPad Prism.

### SUPPLEMENTAL INFORMATION

Supplemental Information includes three figures and one table and can be found with this article online at <http://dx.doi.org/10.1016/j.omtm.2016.12.009>.

### AUTHOR CONTRIBUTIONS

K.-H.C., S.E.S., T.S., K.C., Q.Z., M.L., Y.L., B.F.V., C.S., V.P.H., M.Z., and X.Y. performed experiments and analyzed data. A.R., F.D.U.,

E.J.R., and M.C.H. provided critical reagents and critics. O.D. provided critical insights. J.A.W. performed experiments, analyzed data, and edited the paper. K.-H.C., H.J., and S.T. designed experiments, analyzed data, and wrote the paper.

### CONFLICTS OF INTEREST

K.-H.C., S.E.S., T.S., K.C., Q.Z., J.A.W., M.L., Y.L., B.F.V., C.S., V.P.H., M.Z., S.T., X.Y., and O.D. are or were full-time employees and equity owners of Biogen, and A.R., E.J.R., F.D.U., and M.C.H. are or were full-time employees and equity owners of Sangamo Biosciences when these studies were conducted.

### ACKNOWLEDGMENTS

The authors wish to thank Dr. Bill Hobbs II and Kate Madigan for providing critical insights into  $\beta$  hemoglobinopathies, as well as Attila Fabian and Grigoriy Losyev for flow-activated cell acquisition and sorting.

### REFERENCES

- Manwani, D., and Frenette, P.S. (2013). Vaso-occlusion in sickle cell disease: pathophysiology and novel targeted therapies. *Blood* 122, 3892–3898.
- Telen, M.J. (2016). Beyond hydroxyurea: new and old drugs in the pipeline for sickle cell disease. *Blood* 127, 810–819.
- Pule, G.D., Mowla, S., Novitzky, N., and Wonkam, A. (2016). Hydroxyurea down-regulates BCL11A, KLF-1 and MYB through miRNA-mediated actions to induce  $\gamma$ -globin expression: implications for new therapeutic approaches of sickle cell disease. *Clin. Transl. Med.* 5, 15.
- Steinberg, M.H., Chui, D.H.K., Dover, G.J., Sebastiani, P., and Alsultan, A. (2014). Fetal hemoglobin in sickle cell anemia: a glass half full? *Blood* 123, 481–485.
- Steinberg, M.H., and Sebastiani, P. (2012). Genetic modifiers of sickle cell disease. *Am. J. Hematol.* 87, 795–803.
- Ferrone, F.A. (2016). Sickle cell disease: its molecular mechanism and the one drug that treats it. *Int. J. Biol. Macromol.* 93 (Pt A), 1168–1173.
- Steinberg, M.H., McCarthy, W.F., Castro, O., Ballas, S.K., Armstrong, F.D., Smith, W., Ataga, K., Swerdlow, P., Kutlar, A., DeCastro, L., and Waclawiw, M.A.; Investigators of the Multicenter Study of Hydroxyurea in Sickle Cell Anemia and MSH Patients' Follow-Up (2010). The risks and benefits of long-term use of hydroxyurea in sickle cell anemia: a 17.5 year follow-up. *Am. J. Hematol.* 85, 403–408.
- Voskaridou, E., Christoulas, D., Bilalis, A., Plata, E., Varvagiannis, K., Stamatopoulos, G., Sinopoulou, K., Balassopoulou, A., Loukopoulou, D., and Terpos, E. (2010). The effect of prolonged administration of hydroxyurea on morbidity and mortality in adult patients with sickle cell syndromes: results of a 17-year, single-center trial (LaSHS). *Blood* 115, 2354–2363.
- Wong, T.E., Brandow, A.M., Lim, W., and Lottenberg, R. (2014). Update on the use of hydroxyurea therapy in sickle cell disease. *Blood* 124, 3850–3857, quiz 4004.
- Paulukonis, S.T., Eckman, J.R., Snyder, A.B., Hagar, W., Feuchtbaum, L.B., Zhou, M., Grant, A.M., and Hulihan, M.M. (2016). Defining sickle cell disease mortality using a population-based surveillance system, 2004 through 2008. *Public Health Rep.* 131, 367–375.
- Platt, O.S., Brambilla, D.J., Rosse, W.F., Milner, P.F., Castro, O., Steinberg, M.H., and Klug, P.P. (1994). Mortality in sickle cell disease. Life expectancy and risk factors for early death. *N. Engl. J. Med.* 330, 1639–1644.
- Mentzer, W.C., Heller, S., Pearle, P.R., Hackney, E., and Vichinsky, E. (1994). Availability of related donors for bone marrow transplantation in sickle cell anemia. *Am. J. Pediatr. Hematol. Oncol.* 16, 27–29.
- Alfrah, F., Aljurf, M., Fitzhugh, C.D., and Kassim, A.A. (2016). Alternative donor allogeneic hematopoietic cell transplantation for hemoglobinopathies. *Semin. Hematol.* 53, 120–128.

14. Cavazzana, M., Ribeil, J.-A., Payen, E., Suarez, F., Beuzard, Y., Touzot, F., Cavalleco, R., Lefrere, F., Chretien, S., Bourget, P., et al. (2015). Outcomes of gene therapy for severe sickle disease and beta-thalassemia major via transplantation of autologous hematopoietic stem cells transduced ex vivo with a lentiviral beta AT87Q-globin vector. *Blood* 126, 202.
15. Kanter, J., Walters, M.C., Hsieh, M., Thompson, A.A., Krishnamurti, L., Kwiatkowski, J., Kamble, R.T., von Kalle, C., Kuypers, F.A., Cavazzana, M., et al. (2015). Initial results from study Hgb-206: a phase 1 study evaluating gene therapy by transplantation of autologous CD34+ stem cells transduced ex vivo with the lentiglobin BB305 lentiviral vector in subjects with severe sickle cell disease. *Blood* 126, 3233.
16. Kanter, J., Walters, M.C., Hsieh, M.M., Krishnamurti, L., Kwiatkowski, J., Kamble, R.T., von Kalle, C., Kuypers, F.A., Cavazzana, M., Leboulch, P., et al. (2016). Interim results from a phase 1/2 clinical study of lentiglobin gene therapy for severe sickle cell disease. *Blood* 128, 1176.
17. Sankaran, V.G., Menne, T.F., Xu, J., Akie, T.E., Lettre, G., Van Handel, B., Mikkola, H.K., Hirschhorn, J.N., Cantor, A.B., and Orkin, S.H. (2008). Human fetal hemoglobin expression is regulated by the developmental stage-specific repressor BCL11A. *Science* 322, 1839–1842.
18. Sankaran, V.G., Xu, J., and Orkin, S.H. (2010). Transcriptional silencing of fetal hemoglobin by BCL11A. *Ann. N Y Acad. Sci.* 1202, 64–68.
19. Uda, M., Galanello, R., Sanna, S., Lettre, G., Sankaran, V.G., Chen, W., Usala, G., Busonero, F., Maschio, A., Albai, G., et al. (2008). Genome-wide association study shows BCL11A associated with persistent fetal hemoglobin and amelioration of the phenotype of beta-thalassemia. *Proc. Natl. Acad. Sci. USA* 105, 1620–1625.
20. Xu, J., Sankaran, V.G., Ni, M., Menne, T.F., Puram, R.V., Kim, W., and Orkin, S.H. (2010). Transcriptional silencing of gamma-globin by BCL11A involves long-range interactions and cooperation with SOX6. *Genes Dev.* 24, 783–798.
21. Brendel, C., Guda, S., Renella, R., Du, P., Bauer, D.E., Canver, M.C., Kamran, S.C., Thornton, J., de Boer, H., Milsom, M.D., et al. (2014). Optimization of Bcl11a Knockdown by miRNA scaffold embedded shRNAs leading to enhanced induction of fetal hemoglobin in erythroid cells for the treatment of beta-hemoglobinopathies. *Blood* 124, 2150.
22. Brendel, C., Guda, S., Renella, R., Bauer, D.E., Canver, M.C., Kim, Y.J., Heeney, M.M., Klatt, D., Fogel, J., Milsom, M.D., et al. (2016). Lineage-specific BCL11A knockdown circumvents toxicities and reverses sickle phenotype. *J. Clin. Invest.* 126, 3868–3878.
23. Sebastiano, V., Maeder, M.L., Angstman, J.F., Haddad, B., Khayter, C., Yeo, D.T., Goodwin, M.J., Hawkins, J.S., Ramirez, C.L., Batista, L.F., et al. (2011). In situ genetic correction of the sickle cell anemia mutation in human induced pluripotent stem cells using engineered zinc finger nucleases. *Stem Cells* 29, 1717–1726.
24. Li, C., Ding, L., Sun, C.W., Wu, L.C., Zhou, D., Pawlik, K.M., Khodadadi-Jamayran, A., Westin, E., Goldman, F.D., and Townes, T.M. (2016). Novel HDAd/EBV reprogramming vector and highly efficient Ad/CRISPR-Cas sickle cell disease gene correction. *Sci. Rep.* 6, 30422.
25. Hoban, M.D., Cost, G.J., Mendel, M.C., Romero, Z., Kaufman, M.L., Joglekar, A.V., Ho, M., Lumaquin, D., Gray, D., Lill, G.R., et al. (2015). Correction of the sickle cell disease mutation in human hematopoietic stem/progenitor cells. *Blood* 125, 2597–2604.
26. Dever, D.P., Bak, R.O., Reinisch, A., Camarena, J., Washington, G., Nicolas, C.E., Pavel-Dinu, M., Saxena, N., Wilkens, A.B., Mantri, S., et al. (2016). CRISPR/Cas9  $\beta$ -globin gene targeting in human hematopoietic stem cells. *Nature* 539, 384–389.
27. Lee, J., Dykstra, B., Sackstein, R., and Rossi, D.J. (2015). Progress and obstacles towards generating hematopoietic stem cells from pluripotent stem cells. *Curr. Opin. Hematol.* 22, 317–323.
28. Genovese, P., Schirotti, G., Escobar, G., Di Tomaso, T., Firrito, C., Calabria, A., Moi, D., Mazzieri, R., Bonini, C., Holmes, M.C., et al. (2014). Targeted genome editing in human repopulating hematopoietic stem cells. *Nature* 510, 235–240.
29. Bauer, D.E., and Orkin, S.H. (2011). Update on fetal hemoglobin gene regulation in hemoglobinopathies. *Curr. Opin. Pediatr.* 23, 1–8.
30. Xu, J., Peng, C., Sankaran, V.G., Shao, Z., Esrick, E.B., Chong, B.G., Ippolito, G.C., Fujiwara, Y., Ebert, B.L., Tucker, P.W., and Orkin, S.H. (2011). Correction of sickle cell disease in adult mice by interference with fetal hemoglobin silencing. *Science* 334, 993–996.
31. Canver, M.C., Smith, E.C., Sher, F., Pinello, L., Sanjana, N.E., Shalem, O., Chen, D.D., Schupp, P.G., Vinjamur, D.S., Garcia, S.P., et al. (2015). BCL11A enhancer dissection by Cas9-mediated in situ saturating mutagenesis. *Nature* 527, 192–197.
32. Vierstra, J., Reik, A., Chang, K.H., Stehling-Sun, S., Zhou, Y., Hinkley, S.J., Paschon, D.E., Zhang, L., Psatha, N., Bendana, Y.R., et al. (2015). Functional footprinting of regulatory DNA. *Nat. Methods* 12, 927–930.
33. Bauer, D.E., Kamran, S.C., Lessard, S., Xu, J., Fujiwara, Y., Lin, C., Shao, Z., Canver, M.C., Smith, E.C., Pinello, L., et al. (2013). An erythroid enhancer of BCL11A subject to genetic variation determines fetal hemoglobin level. *Science* 342, 253–257.
34. Hu, J., Liu, J., Xue, F., Halverson, G., Reid, M., Guo, A., Chen, L., Raza, A., Galili, N., Jaffray, J., et al. (2013). Isolation and functional characterization of human erythroblasts at distinct stages: implications for understanding of normal and disordered erythropoiesis in vivo. *Blood* 121, 3246–3253.
35. Luc, S., Huang, J., McEldoon, J.L., Somuncular, E., Li, D., Rhodes, C., Mamoor, S., Hou, S., Xu, J., and Orkin, S.H. (2016). Bcl11a deficiency leads to hematopoietic stem cell defects with an aging-like phenotype. *Cell Rep.* 16, 3181–3194.
36. Tsang, J.C., Yu, Y., Burke, S., Buettner, F., Wang, C., Kolodziejczyk, A.A., Teichmann, S.A., Lu, L., and Liu, P. (2015). Single-cell transcriptomic reconstruction reveals cell cycle and multi-lineage differentiation defects in Bcl11a-deficient hematopoietic stem cells. *Genome Biol.* 16, 178.
37. Poillon, W.N., Kim, B.C., Rodgers, G.P., Noguchi, C.T., and Schechter, A.N. (1993). Sparing effect of hemoglobin F and hemoglobin A2 on the polymerization of hemoglobin S at physiologic ligand saturations. *Proc. Natl. Acad. Sci. USA* 90, 5039–5043.
38. Steinberg, M.H., and Rodgers, G.P. (2001). Pathophysiology of sickle cell disease: role of cellular and genetic modifiers. *Semin. Hematol.* 38, 299–306.
39. Thein, S.L. (2011). Genetic modifiers of sickle cell disease. *Hemoglobin* 35, 589–606.
40. Eaton, W.A., and Hofrichter, J. (1987). Hemoglobin S gelation and sickle cell disease. *Blood* 70, 1245–1266.
41. Lettre, G., Sankaran, V.G., Bezerra, M.A., Araújo, A.S., Uda, M., Sanna, S., Cao, A., Schlessinger, D., Costa, F.F., Hirschhorn, J.N., and Orkin, S.H. (2008). DNA polymorphisms at the BCL11A, HBS1L-MYB, and beta-globin loci associate with fetal hemoglobin levels and pain crises in sickle cell disease. *Proc. Natl. Acad. Sci. USA* 105, 11869–11874.
42. Menzel, S., Garner, C., Gut, I., Matsuda, F., Yamaguchi, M., Heath, S., Foglio, M., Zelenika, D., Boland, A., Rooks, H., et al. (2007). A QTL influencing F cell production maps to a gene encoding a zinc-finger protein on chromosome 2p15. *Nat. Genet.* 39, 1197–1199.
43. Thein, S.L., Menzel, S., Peng, X., Best, S., Jiang, J., Close, J., Silver, N., Gerovasilli, A., Ping, C., Yamaguchi, M., et al. (2007). Intergenic variants of HBS1L-MYB are responsible for a major quantitative trait locus on chromosome 6q23 influencing fetal hemoglobin levels in adults. *Proc. Natl. Acad. Sci. USA* 104, 11346–11351.
44. Traxler, E.A., Yao, Y., Wang, Y.D., Woodard, K.J., Kurita, R., Nakamura, Y., Hughes, J.R., Hardison, R.C., Blobel, G.A., Li, C., and Weiss, M.J. (2016). A genome-editing strategy to treat  $\beta$ -hemoglobinopathies that recapitulates a mutation associated with a benign genetic condition. *Nat. Med.* 22, 987–990.
45. Ye, L., Wang, J., Tan, Y., Beyer, A.L., Xie, F., Muench, M.O., and Kan, Y.W. (2016). Genome editing using CRISPR-Cas9 to create the HFPFH genotype in HSPCs: An approach for treating sickle cell disease and  $\beta$ -thalassemia. *Proc. Natl. Acad. Sci. USA* 113, 10661–10665.
46. Bjurstrom, C.F., Mojadidi, M., Phillips, J., Kuo, C., Lai, S., Lill, G.R., Cooper, A., Kaufman, M., Urbinati, F., Wang, X., et al. (2016). Reactivating fetal hemoglobin expression in human adult erythroblasts through BCL11A knockdown using targeted endonucleases. *Mol. Ther. Nucleic Acids* 5, e351.
47. Fitzhugh, C.D., Hsieh, M.M., Bolan, C.D., Saenz, C., and Tisdale, J.F. (2009). Granulocyte colony-stimulating factor (G-CSF) administration in individuals with sickle cell disease: time for a moratorium? *Cytotherapy* 11, 464–471.
48. Sankaran, V.G., Xu, J., Ragozy, T., Ippolito, G.C., Walkley, C.R., Maika, S.D., Fujiwara, Y., Ito, M., Groudine, M., Bender, M.A., et al. (2009). Developmental and species-divergent globin switching are driven by BCL11A. *Nature* 460, 1093–1097.
49. Liu, P., Keller, J.R., Ortiz, M., Tessoro, L., Rachel, R.A., Nakamura, T., Jenkins, N.A., and Copeland, N.G. (2003). Bcl11a is essential for normal lymphoid development. *Nat. Immunol.* 4, 525–532.

50. Noguchi, C.T., Rodgers, G.P., Serjeant, G., and Schechter, A.N. (1988). Levels of fetal hemoglobin necessary for treatment of sickle cell disease. *N. Engl. J. Med.* *318*, 96–99.
51. Funnell, A.P., Prontera, P., Ottaviani, V., Piccione, M., Giambona, A., Maggio, A., Ciaffoni, F., Stehling-Sun, S., Marra, M., Masiello, F., et al. (2015). 2p15-p16.1 microdeletions encompassing and proximal to BCL11A are associated with elevated HbF in addition to neurologic impairment. *Blood* *126*, 89–93.
52. Basak, A., Hancarova, M., Ulirsch, J.C., Balci, T.B., Trkova, M., Pelisek, M., Vlkova, M., Muzikova, K., Cermak, J., Trka, J., et al. (2015). BCL11A deletions result in fetal hemoglobin persistence and neurodevelopmental alterations. *J. Clin. Invest.* *125*, 2363–2368.
53. Fixler, J., Vichinsky, E., and Walters, M.C. (2001). Stem cell transplantation for sickle cell disease: can we reduce the toxicity? *Pediatr. Pathol. Mol. Med.* *20*, 73–86.
54. Walters, M.C., and Sullivan, K.M. (2010). Stem-cell transplantation for sickle cell disease. *N. Engl. J. Med.* *362*, 955–956, author reply 956.
55. Kean, L.S., Mancini, E.A., Perry, J., Balkan, C., Coley, S., Holtzclaw, D., Adams, A.B., Larsen, C.P., Hsu, L.L., and Archer, D.R. (2003). Chimerism and cure: hematologic and pathologic correction of murine sickle cell disease. *Blood* *102*, 4582–4593.
56. Iannone, R., Luznik, L., Engstrom, L.W., Tennessee, S.L., Askin, F.B., Casella, J.F., Kickler, T.S., Goodman, S.N., Hawkins, A.L., Griffin, C.A., et al. (2001). Effects of mixed hematopoietic chimerism in a mouse model of bone marrow transplantation for sickle cell anemia. *Blood* *97*, 3960–3965.
57. Roberts, C., Kean, L., Archer, D., Balkan, C., and Hsu, L.L. (2005). Murine and math models for the level of stable mixed chimerism to cure beta-thalassemia by nonmyeloablative bone marrow transplantation. *Ann. N Y Acad. Sci.* *1054*, 423–428.
58. Altrock, P.M., Brendel, C., Renella, R., Orkin, S.H., Williams, D.A., and Michor, F. (2016). Mathematical modeling of erythrocyte chimerism informs genetic intervention strategies for sickle cell disease. *Am. J. Hematol.* *91*, 931–937.
59. Donnenberg, A.D., Donnenberg, V.S., Griffin, D.L., Moore, L.R., Tekinturhan, F., and Kormos, R.L. (2011). Intra-operative preparation of autologous bone marrow-derived CD34-enriched cellular products for cardiac therapy. *Cytherapy* *13*, 441–448.
60. Giarratana, M.C., Kobari, L., Lapillonne, H., Chalmers, D., Kiger, L., Cynober, T., Marden, M.C., Wajcman, H., and Douay, L. (2005). Ex vivo generation of fully mature human red blood cells from hematopoietic stem cells. *Nat. Biotechnol.* *23*, 69–74.
61. Thorpe, S.J., Thein, S.L., Sampietro, M., Craig, J.E., Mahon, B., and Huehns, E.R. (1994). Immunochemical estimation of haemoglobin types in red blood cells by FACS analysis. *Br. J. Haematol.* *87*, 125–132.
62. Schroeder, W.A., Shelton, J.B., Shelton, J.R., Huynh, V., and Teplow, D.B. (1985). High performance liquid chromatographic separation of the globin chains of non-human hemoglobins. *Hemoglobin* *9*, 461–482.
63. Lee, J.C., Gimm, J.A., Lo, A.J., Koury, M.J., Krauss, S.W., Mohandas, N., and Chasis, J.A. (2004). Mechanism of protein sorting during erythroblast enucleation: role of cytoskeletal connectivity. *Blood* *103*, 1912–1919.
64. Bell, A.J., Satchwell, T.J., Heesom, K.J., Hawley, B.R., Kupzig, S., Hazell, M., Mushens, R., Herman, A., and Toye, A.M. (2013). Protein distribution during human erythroblast enucleation in vitro. *PLoS ONE* *8*, e60300.
65. Zhang, J., Kobert, K., Flouri, T., and Stamatakis, A. (2014). PEAR: a fast and accurate Illumina Paired-End reAd mergeR. *Bioinformatics* *30*, 614–620.